Supporting Information for:

Room Temperature Electrocaloric Effect in Layered Ferroelectric CuInP$_2$S$_6$ for Solid State Refrigeration

Mengwei Si[1,4], Atanu K. Saha[1], Pai-Ying Liao[1,4], Shengjie Gao[2,4], Sabine M. Neumayer[5], Jie Jian[3], Jingkai Qin[1,4], Nina Balke Wisinger[5], Haiyan Wang[3], Petro Maksymovych[5], Wenzhuo Wu[2,4], Sumeet K. Gupta[1] and Peide D. Ye[1,4,*]

[1] *School of Electrical and Computer Engineering, Purdue University, West Lafayette, Indiana 47907, United States*

[2] *School of Industrial Engineering, Purdue University, West Lafayette, Indiana 47907, United States*

[3] *School of Materials Science and Engineering, Purdue University, West Lafayette, In 47907, United States*

[4] *Birck Nanotechnology Center, Purdue University, West Lafayette, Indiana 47907, United States*

[5] *Center for Nanophase Materials Sciences, Oak Ridge National Laboratory, Bethel Valley Road, Oak Ridge, Tennessee 37831, United States*

* Address correspondence to: yep@purdue.edu (P.D.Y.)

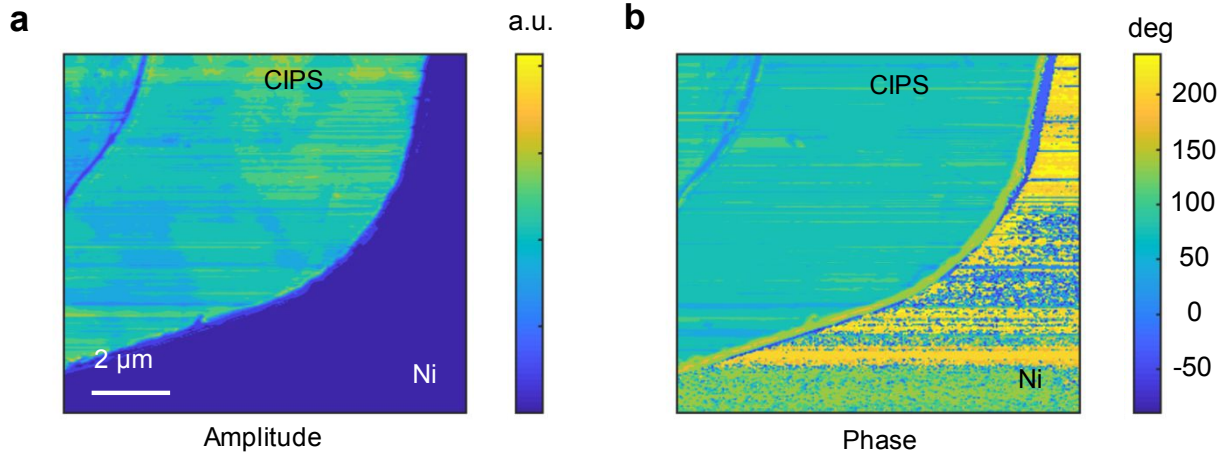1

1. DART-PFM measurement on CIPS thin film

Figure S1. (a) PFM amplitude and (b) PFM phase images of CIPS flake on a Ni/SiO₂/Si substrate by DART-PFM, showing clear piezoelectric response.

Fig. S1(a) and S1(b) show the phase and amplitude by DART-PFM, suggesting a clear piezoelectric response in CIPS thin film. Fig. S2 shows the raw data of single point DART-PFM hysteresis loop measurement at 310 K. Fig. S2(a) shows the applied voltage biases versus time. Three cycles of triangular voltage waves are applied with both on field and off field PFM measurements, as shown in Fig. S2(b). Fig. S2(c)-(d) show the PFM amplitude, phase1 and phase2 signals. A clear ferroelectric polarization switching can be seen on both phase1 and phase2 signals, at both on field and off field. The raw data itself confirms the ferroelectricity of CIPS at 310 K. Fig. S3(a)-(c) show the PFM amplitude, phase1 and phase2 signals of CIPS measured at 325 K. The biases and time sequences are same as in Fig. S2(a). No ferroelectric phase switching can be seen on both phase1 and phase2 signals at off field, suggesting the loss of ferroelectricity of CIPS at 325 K. Further thickness-dependent PFM measurements are performed at room temperature to explore the scaling property of ferroelectric CIPS. As shown

in the thickness-dependent PFM measurements on CIPS in Fig. S4 from 140 nm down to 15 nm, clear ferroelectric hysteresis loop can be achieved down to 40 nm, suggesting the stable ferroelectricity in CIPS down to tens of nm at room temperature.
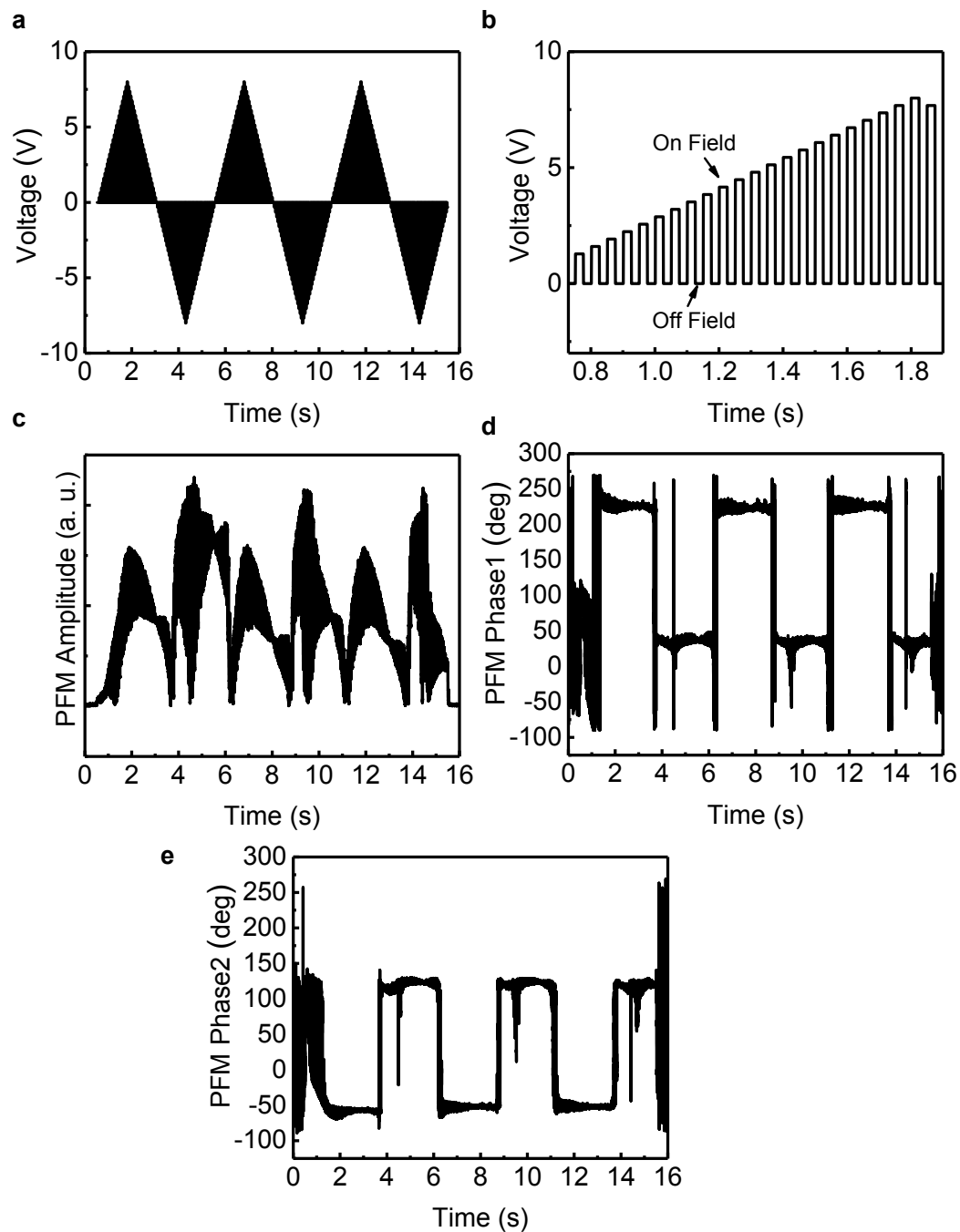
Figure S2. Raw data of single point DART-PFM hysteresis loop measurements at 310 K. (a) Bias, (b) zoom-in plot of (a), showing on field and off field measurements, (c) amplitude, (d) phase1, and (e) phase2.
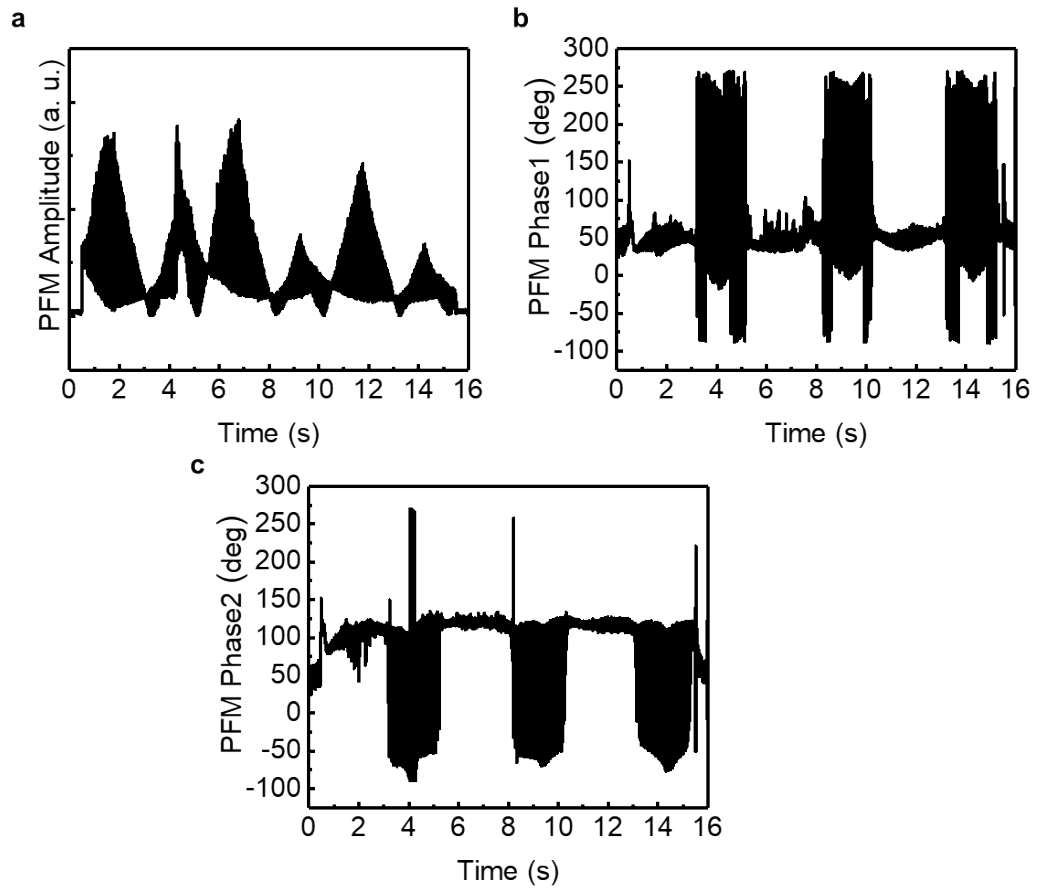
Figure S3. Raw data of single point DART-PFM hysteresis loop measurements at 325 K. (a) Amplitude, (b) phase1, and (c) phase2.
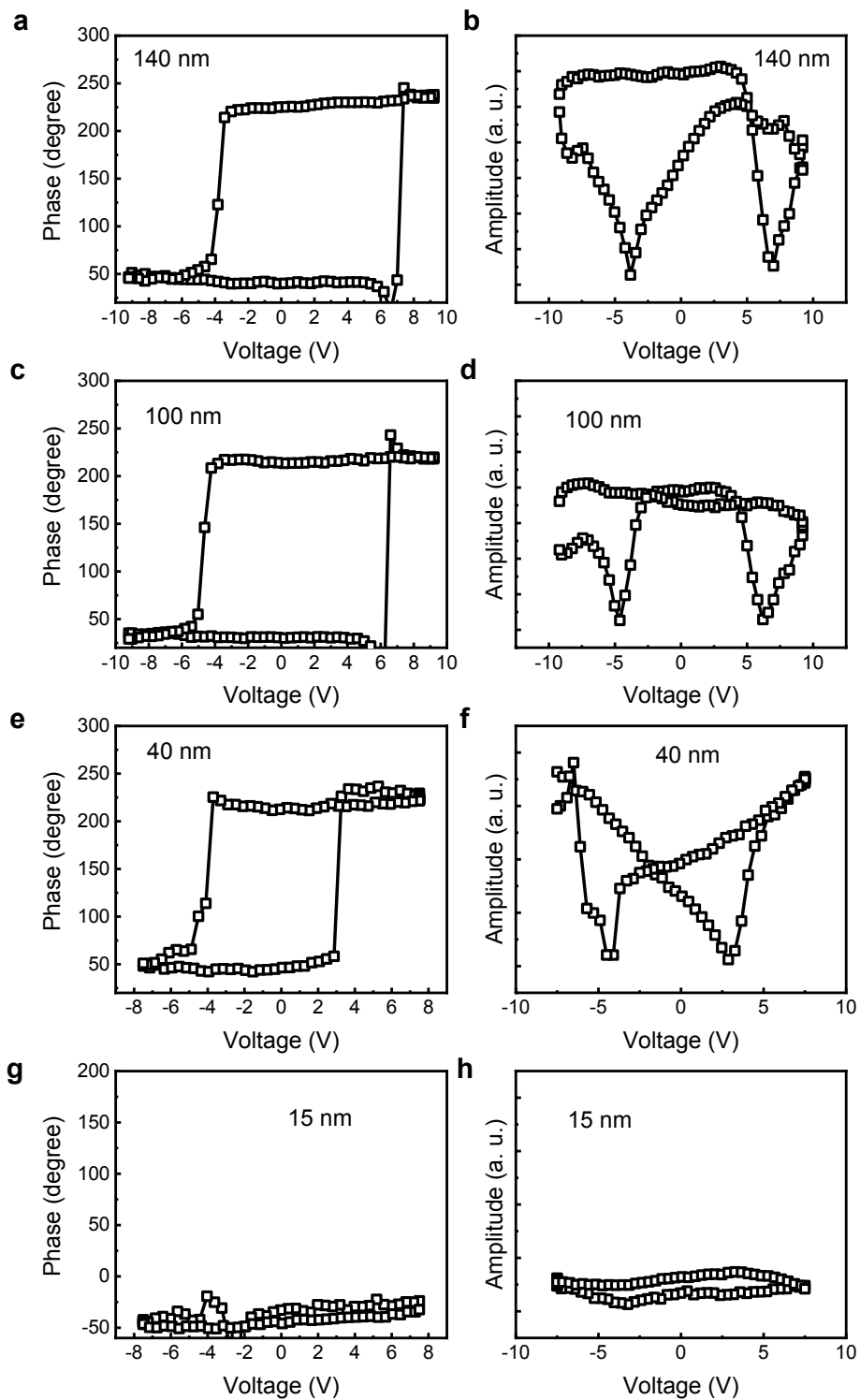
Figure S4. Thickness dependent PFM measurements on CIPS at room temperature. Phase versus voltage hysteresis loop at (a) 140 nm, (c) 100 nm, (e) 40 nm and (g) 15 nm. Amplitude versus voltage hysteresis loop at (b) 140 nm, (d) 100 nm, (f) 40 nm and (h) 15 nm.

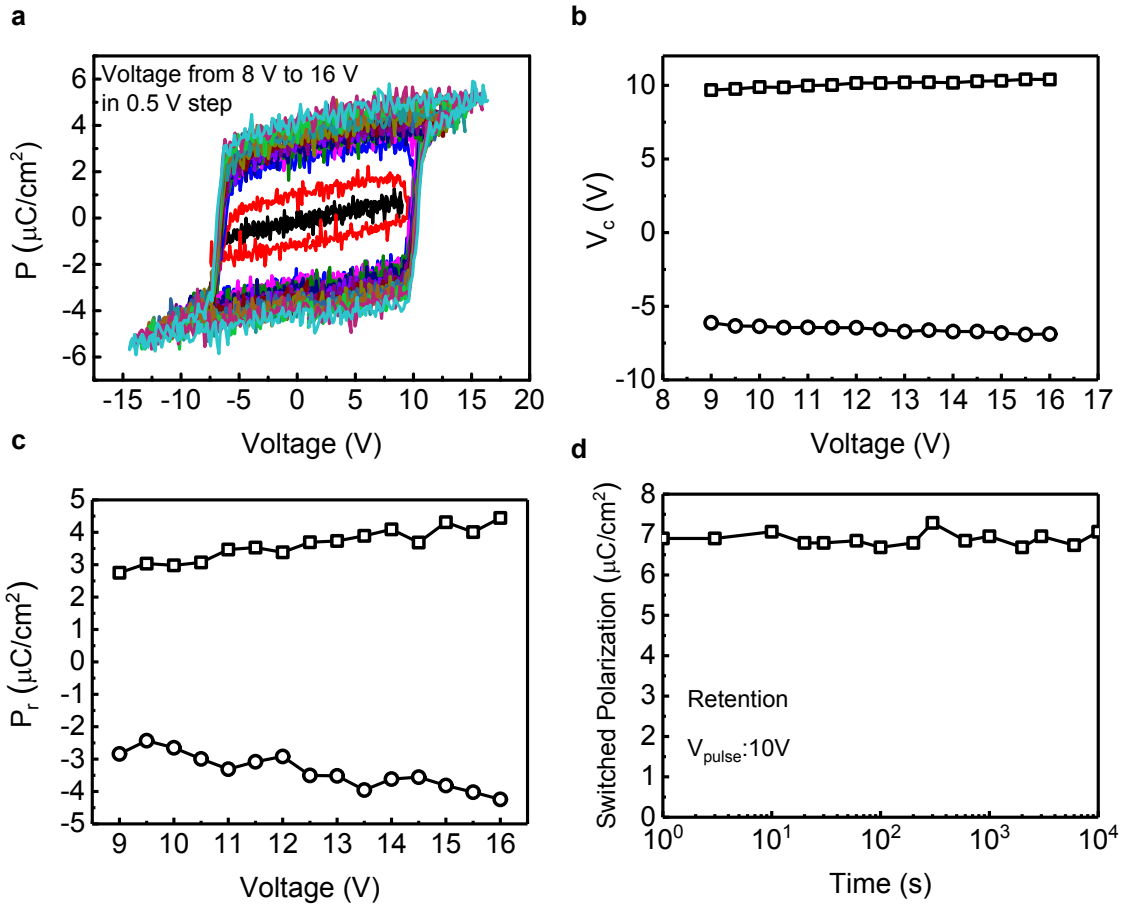## 2. Voltage-dependent ferroelectricity and ferroelectric retention

Figure S5. (a) P-V hysteresis loop of CIPS capacitor at different voltage sweep ranges. (b) Coercive voltage and (c) remnant polarization versus sweep voltages. (d) Switched polarization versus time in ferroelectric retention measurement, showing retention-free up to 10^4 s.

Fig. S5(a) shows voltage-dependent P-V hysteresis loop of CIPS capacitor. Fig. S5(b) shows the coercive voltage (V_c) versus maximum applied voltages. Fig. S5(c) shows the remnant polarization (P_r) versus maximum applied voltages. Fig. S5(d) shows the polarization retention measurement of CIPS capacitor. No polarization retention is observed up to 10^4 s.

3. Modelling and Calibration:

To simulate the electrocaloric effect in CIPS, we solve the temperature (T) dependent Landau-Khalatnikov equation (eqn. (1)) that captures the relation among polarization, temperature and applied electric field.

$$E - \rho_{FE}\frac{dP}{dt} = \alpha_0(T - T_0)P + \beta P^3 + \gamma P^5 \qquad (1)$$

Here, P is the polarization, E is the applied electric field, ρ_{FE} is the viscosity coefficient and t is time. α_0, β and γ are Landau coefficients and T_0 is the Curie-Weiss temperature. According to eqn. (1), the temperature driven phase transition depends on the sign of β. For $\beta>0$, eqn. (1) can capture the second order phase transition and if $\beta<0$, then the equation corresponds to the first order phase transition. In case of second order phase transition, the Curie temperature (T_C) is the same as T_0. At $T=T_C=T_0$, the material changes its phase from FE to PE.
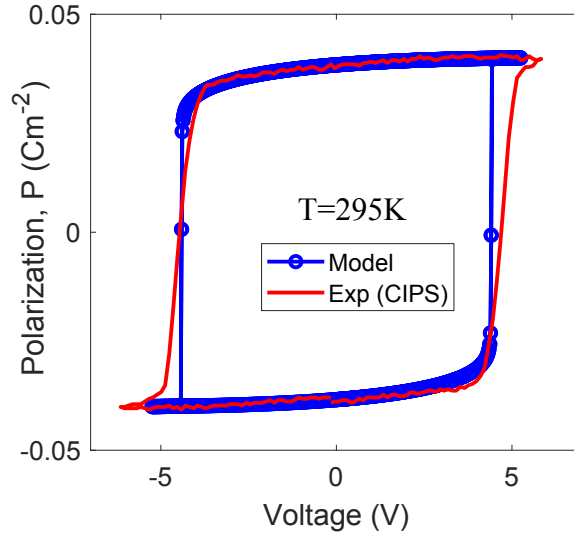

Figure S6. Experimentally measured and simulated P-V hysteresis loop of CIPS capacitor at T=295 K.

We calibrate the Landau coefficients by fitting the simulated polarization versus voltage (P-V) characteristics with the measured P-V characteristics for T=295 K (Fig. S6). As the

8

experimentally measured temperature dependent P-V characteristics suggest second order phase transition in CIPS, therefore, we assume $\beta > 0$, in our calibration. The corresponding Landau coefficients we get from the calibration are presented in Table SI. Then, the electrocaloric temperature change can be calculated using eqn. (2) based on the simulated temperature dependent P-V characteristics, where C is the heat capacity, ρ is the mass density.

$$\Delta T = - \int_{E_1}^{E_2} \frac{1}{C\rho} T \left(\frac{\partial P}{\partial T}\right)_E dE \tag{2}$$

Table - SI: Landau coefficients considering the second order phase transition (CIPS, T=295 K, T_0=315 K)

$\alpha_0(T-T_0)$	-3.52×10^8 m/F
β	1.38×10^{11} m^5/F/C^2
γ	6.81×10^{13} m^9/F/C^4

4. Benchmarking of EC Materials:

Table SII shows the performance of selected EC materials according to Ref. 1. CIPS exhibits comparable EC performance with other 3D EC materials. Note that comparing with most thin film ferroelectric materials, such as thin film PZT[4], PMN-PT[6], SBT[7], P(VDF-TrFE)[8], the EC strength ($|\Delta T|/|\Delta E|$) of CIPS is quite high.

Note that ΔT is proportional to $\partial P/\partial T$ according to eqn. (2). $\partial P/\partial T$ can be further estimated as $P_r \partial P_\% /\partial T$, where P_r is the remnant polarization and $\partial P_\% /\partial T$ is the slope of polarization percentage change. This means if CIPS has a remnant polarization of ~30-40 $\mu C/cm^2$ (similar to conventional ferroelectric materials like PZT) while maintaining the same slope of polarization percentage change, a $|\Delta T|$ of over 30 K can be achieved. This is a very high number comparing with other EC materials.

Table - SII: Performance of Selected EC Materials

EC Material	T (K)	$|\Delta T|$ (K)	$|\Delta E|$ (kV cm^{-1})	$|\Delta T|/|\Delta E|$ (mK cm kV^{-1})	Ref.
KH_2PO_4	123	1.0	10	100	2
$BaTiO_3$	397	0.9	4	225	3
$PbZr_{0.95}Ti_{0.05}O_3$	499	12	480	25	4
$Pb_{0.8}Ba_{0.2}ZrO_3$	290	45	598	75.3	5
0.9PMN-0.1PT	348	5.0	895	5.6	6
$SrBi_2Ta_2O_9$	565	4.9	600	8.2	7
P(VDF-TrFE)	323	28	1800	15.6	8
CIPS (This work)	315	3.3	142	29.5	

References

1. Moya, X.; Kar-Narayan, S.; Mathur, N. D. Caloric Materials near Ferroic Phase Transitions. *Nat. Mater.* **2014**, *13*, 439–450.
2. Baumgartner, H. Elektrische Sättigungserscheinungen und Elektrokalorischer Effekt von Kaliumphosphat KH_2PO_4. *Helv. Phys. Acta* **1950**, *23*, 651–696.
3. Moya, X.; Stern-Taulats, E.; Crossley, S.; Gonzá lez-Alonso, D.; Kar-Narayan, S.; Planes, A.; Mañosa, L.; Mathur, N. D. Giant Electrocaloric Strength in Single‑Crystal $BaTiO_3$. *Adv. Mater.* **2013**, *25*, 1360–1365.
4. Mischenko A. S.; Zhang Q.; Scott J. F.; Whatmore R. W.; Mathur N. D. Giant Electrocaloric Effect in Thin-Film $PbZr_{0.95}Ti_{0.05}O_3$. *Science* **2006**, *311*, 1270–1271.
5. Peng, B.; Fan, H.; Zhang, Q. A Giant Electrocaloric Effect in Nanoscale Antiferroelectric and Ferroelectric Phases Coexisting in a Relaxor $Pb_{0.8}Ba_{0.2}ZrO_3$ Thin Film at Room Temperature. *Adv. Funct. Mater.* **2013**, *23*, 2987–2992.
6. Mischenko, A. S.; Zhang, Q.; Whatmore, R. W.; Scott, J. F.; Mathur, N. D. Giant Electrocaloric Effect in the Thin Film Relaxor Ferroelectric 0.9 $PbMg_{1/3}Nb_{2/3}O_3$-0.1 $PbTiO_3$ near Room Temperature. *Appl. Phys. Lett.* **2006**, 89, 242912.
7. Chen, H.; Ren, T.-L.; Wu, X.-M.; Yang, Y.; Liu, L.-T. Giant Electrocaloric Effect in Lead-Free Thin Film of Strontium Bismuth Tantalite. *Appl. Phys. Lett.* **2009**, *94*, 182902.
8. Li, X.; Qian, X.-S.; Gu, H.; Chen, X.; Lu, S. G.; Lin, M.; Bateman, F.; Zhang, Q. M. Giant Electrocaloric Effect in Ferroelectric Poly(vinylidenefluoride-trifluoroethylene) Copolymers near a First-Order Ferroelectric Transition. *Appl. Phys. Lett.* **2012**, *101*, 132903.